All objects and some questions

Charles H. Lineweaver[a] and Vihan M. Patel[b]
Research School of Astronomy and Astrophysics, Australian National University, Canberra 2600, Australia

(Received 13 March 2023; accepted 8 August 2023)

We present an overview of the thermal history of the Universe and the sequence of objects (e.g., protons, planets, and galaxies) that condensed out of the background as the Universe expanded and cooled. We plot (i) the density and temperature of the Universe as a function of time and (ii) the masses and sizes of all objects in the Universe. These comprehensive pedagogical plots draw attention to the triangular regions forbidden by general relativity and quantum uncertainty and help navigate the relationship between gravity and quantum mechanics. How can we interpret their intersection at the smallest possible objects: Planck-mass black holes ("instantons")? Does their Planck density and Planck temperature make them good candidates for the initial conditions of the Universe? Our plot of all objects also seems to suggest that the Universe is a black hole. We explain how this depends on the unlikely assumption that our Universe is surrounded by zero density Minkowski space.
https://doi.org/10.1119/5.0150209

I. INTRODUCTION

A. Condensation of objects

The early Universe was a hot plasma of fundamental relativistic particles: quarks, leptons, photons, and gluons. There were no composite objects such as protons, atoms, planets, or galaxies.[1–5] As the Universe cooled, composite objects condensed out of the background much as droplets of steam condense out of hot water vapor as it cools. This condensation happened when the binding energy of an object exceeded the background energy. For example, as the Universe expanded and cooled during the quark-hadron transition, the binding energy of the strong force overcame the background energy as the quark-gluon plasma condensed into protons, neutrons, and other hadrons. With further expansion and decrease in temperature, during the epoch of big bang nucleosynthesis, the binding energy of the residual strong force overcame the background energy as the hot plasma of protons and neutrons condensed into atomic nuclei. Further expansion and cooling led to the formation of helium and then hydrogen atoms when the binding energy of coulomb forces overcame the background energy. With further cooling, chemical bond energies overcame the kinetic energy of atoms as they condensed into molecules. Further cooling allowed matter-overdensities to form stars, planets, galaxies, and clusters of galaxies as their gravitational binding energy overcame their kinetic energy.[1,2]

As a result of this sequence of condensations, due to the strong force, electromagnetism, and gravity, the Universe is now filled with protons, atoms, molecules, stars, planets, black holes, and galaxies whose densities are higher than the current average density of the Universe. These condensations can also be described as first-order symmetry-breaking phase transitions from a disordered higher symmetry hot phase to a more ordered lower symmetry cooler phase.[3,4] To help quantify the context for this sequence of transitions, we compute and plot (Fig. 1) the time dependence of the decreasing density and temperature of the Universe.

B. Changing dominant densities in the Universe

Starting with inflation, the dominant densities have been the densities of the false vacuum energy of inflation (Ω_{Λ_i}), radiation (Ω_r), matter (Ω_m), and finally today, vacuum energy or dark energy (Ω_Λ). The three transitions among these four epochs are known, respectively, as reheating, matter-radiation equality, and the beginning of vacuum energy domination.

The details of inflation are largely unknown.[3,12] For simplicity, we assume the initial condition at the Planck time that the Universe was at the Planck temperature and the Planck density (t_p, T_p, and ρ_p, respectively). We assume the Universe underwent inflationary expansion[13–15] that ended at the grand unified theory (GUT) scale ($t \sim 10^{-32}$ s) when reheating produced a radiation-dominated Universe with an energy density equal to the energy density during inflation: $\rho_{GUT} = \rho_{\Lambda_i}$.[16] Following Refs. 1 and 17, we also assume radiation domination before inflation. These assumptions constrain inflation to start at $t \sim 10^{-36}$ s.

As the Universe expanded, the scalefactor (a) increased. Since the density of radiation $\rho_r \propto a^{-4}$, while the density of matter $\rho_m \propto a^{-3}$, expansion led to matter-radiation equality: $\rho_r \sim \rho_m$. After equality, the Universe became matter dominated and gravity, like the other stronger forces before it, could begin to condense or accrete objects out of the background.

C. Relativistic degrees of freedom in the early Universe: g_*

A couple of minutes after the big bang ($t \gtrsim 10^2$ s), as the Universe expanded and the scale factor of the Universe increased, the average temperature of the photons filling the Universe decreased according to Eq. (1). If we want the temperature at earlier times, the more general Eq. (2) is needed. It depends on both the scale factor and on g_*, the number of relativistic degrees of freedom in thermal equilibrium with the photons[1,3,18]

$$T = T_o\, a^{-1} \quad \text{for } t \gtrsim 10^2\,\text{s}, \tag{1}$$

$$T = T_o\, a^{-1} \left(\frac{g_*}{2}\right)^{-1/3}, \tag{2}$$

where $T_o = 2.725$ K is the temperature of the current cosmic microwave background (CMB) photons.[19] The g_* in Eq. (2)

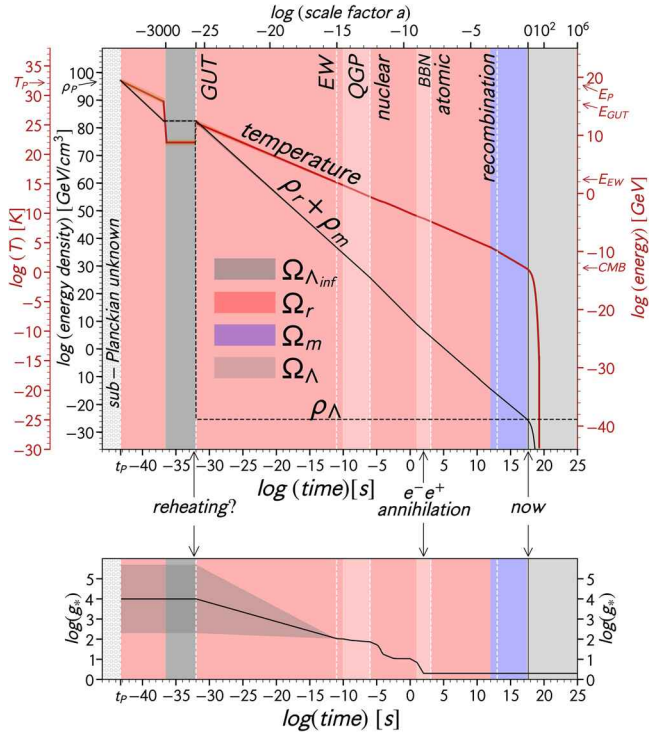

Fig. 1. (Color online) Top panel: The decreasing average temperature and density of the Universe as a function of time (and on the upper x-axis as a function of scale factor a). The solid black line is the energy density of radiation and matter ($\rho_r + \rho_m$). The dashed black line is the energy density of the vacuum. The red line is the average temperature of the Universe. The background is color-coded to show the densities that dominate the Universe as a function of time. From left to right starting at the Planck time, the dominant densities are: pink (radiation, Ω_r), grey (false vacuum energy of inflation, Ω_{Λ_i}), pink (radiation, Ω_r), blue (matter, Ω_m), and light grey (vacuum energy or dark energy, Ω_Λ). The transition from the matter domination to the current dark energy domination occurred at $t \approx 2.4 \times 10^{17}$s after the big bang (about 6.1×10^9 years ago). Because of the logarithmic time axis, this transition is barely distinguishable to the left of the vertical "now" line (4.4×10^{17} s). This plot assumes a ΛCDM Universe with $\Omega_m = 0.30 \pm 0.02$, $\Omega_\Lambda = 0.70 \pm 0.02$, $H_o = 70 \pm 2\,\mathrm{km\,s^{-1}Mpc^{-1}}$. "GUT" is the energy scale of grand unified theories, "EW" is the electroweak energy scale, "QGP" is the epoch of quark-gluon plasma while "BBN" is the epoch of big bang nucleosynthesis. Bottom panel: The effective number of relativistic degrees of freedom g_* as a function of time. Estimates of g_* for times $t \gtrsim 10^{-10}$ s are from Refs. 1 and 6–9. At $t \sim 10^{-10}$ s, the particles of the standard model are relativistic and produce 106.75 degrees of freedom. The large uncertainty in g_* for $t \lesssim 10^{-10}$ s is the notional range taken from Ref. 6. At these earlier times and higher energies, the values of g_* are poorly constrained and depend on the model of high energy particle physics (Refs. 1 and 10). The values of g_* in the bottom panel, when inserted into Eqs. (2) and (5) produce the temperatures and energy densities in the top panel. To be explicit and simple, we have assumed $g_*(t < 10^{-32}\mathrm{s}) = g_*(t = 10^{-32}\mathrm{s})$. Times before the Planck time are labelled "sub-Planckian unknown." On any log(time) axis, $t = 0$ is infinitely far to the left. This choice precludes all models in which time has no beginning (e.g., Ref. 11).

can be thought of as a measure of the heat capacity of the hot relativistic plasma. It is analogous to the number of degrees of freedom of a polyatomic gas. As the temperature increases, more vibrational and rotational degrees of freedom become available. Energy added to the system has to be partitioned among the increasing number of degrees of freedom, rather than directly increasing the temperature of the system. With more degrees of freedom, the heat capacity of the gas increases.

Similarly, as we go back in time (before $t \sim 10^2$ s) to the increasingly high energies of the early Universe, g_* increases as the two degrees of freedom of photons are joined in thermal equilibrium by the degrees of freedom of the increasingly numerous relativistic particles. Hot relativistic particles act like massless photons since their energy, $E = (p^2c^2 + m^2c^4)^{1/2}$ is dominated by their momentum and can be well-approximated by $E \approx pc$. As we go back in time, getting closer to the big bang, g_* increases. Thus, we need to replace Eq. (1) with Eq. (2), from which we can see that as we get closer to the big bang, T does not increase as fast as $\sim a^{-1}$. In the lower panel of Fig. 1, we can see that g_* begins to increase for $t \lesssim 10^2$ s. If photons are the only form of radiation, Eqs. (1) and (2) are identical since $g_* = 2$ (one degree of freedom for each of the two photon spin states).

Currently, neutrinos are not in thermal equilibrium with the 3 K photons of the cosmic microwave background. The relativistic degrees of freedom of neutrinos are not included in our g^* for temperatures $T \lesssim 10^{10}$K when they are decoupled from photons.

Similar to temperature in Eq. (2), the energy density ρ_r of a relativistic gas also depends on g_*. If we only have photons, the energy density is given in Eq. (3). However, if there are other relativistic particles in thermal equilibrium with photons at a common temperature T, to compute their combined energy density we need to multiply Eq. (3) by $g_*/2$ to obtain the generalization Eq. (4).[1,7,8] Finally, using Eq. (2), we substitute for T in Eq. (4) and obtain Eq. (5): the energy density in all relativistic degrees of freedom (in thermal equilibrium with photons) as a function of scale factor and g_*,[3,12]

$$\rho_r = a_B \quad T^4 \quad \text{for } t \gtrsim 10^2\,\mathrm{s}, \tag{3}$$

$$\rho_r = a_B \quad T^4 \quad \left(\frac{g_*}{2}\right), \tag{4}$$

$$\rho_r = a_B \left(\frac{T_o}{a}\right)^4 \left(\frac{g_*}{2}\right)^{-1/3}, \tag{5}$$

where the radiation density constant $a_B = (\pi^2 k^4/15\,\hbar^3 c^3)$.[3] Comparing Eqs. (2) and (5), we see that both temperature and density have the same $g_*^{-1/3}$ dependence. Inserting the $g*$ of the lower panel of Fig. 1 into Eqs. (2) and (5) enables us to plot in the upper panel of Fig. 1 the time dependence of the background temperature and density during the condensation of objects in the Universe.

II. PLOT OF ALL OBJECTS

A. Objects and isodensity lines

In Fig. 2, we plot all the composite objects in the Universe: protons, atoms, life forms, asteroids, moons, planets, stars, galaxies, galaxy clusters, giant voids, and the Universe itself. Humans are represented by a mass of 70 kg and a radius of 50 cm (we assume sphericity), while whales are represented by a mass of 10^5 kg and a radius of 7 m. Objects with uniform density ρ are described by $m \propto \rho\, r^3$. Thus, in a log(m)–log(r) plot such as Fig. 2, all objects of the same density fall along the same isodensity line of slope 3. For example, atoms and objects made of atoms, such as life on Earth (viruses, bacteria, fleas, humans, and whales) asteroids, moons, planets, and main sequence stars, lie close to the atomic density line $\rho_{atomic} \sim \rho_{water} = 1\,\mathrm{gm/cm^3}$. At the top of the plot, this line is labeled "atomic 10^3s," because

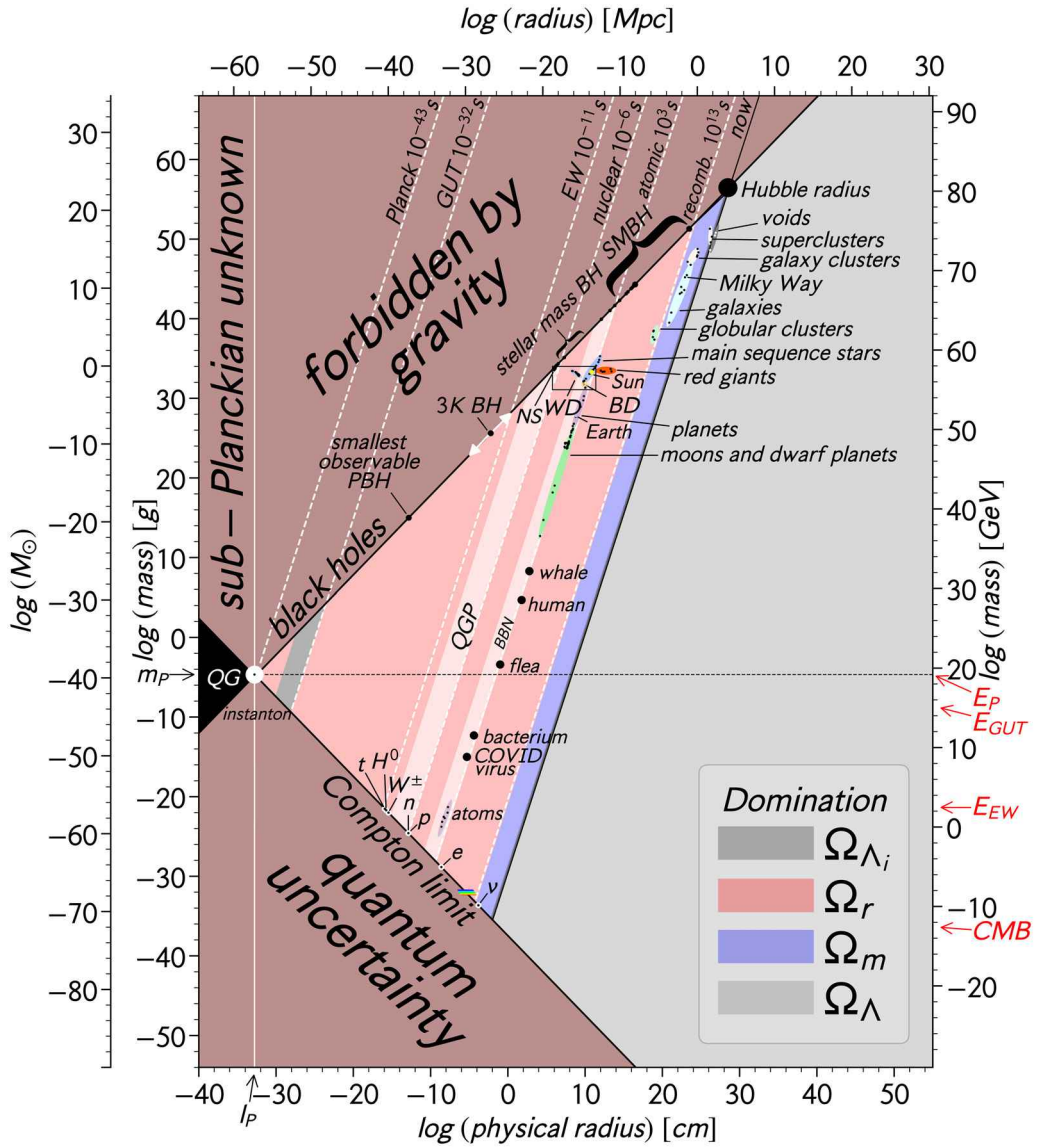

Fig. 2. (Color online) Masses, sizes, and relative densities of objects in our Universe. Time-dependent background densities are color-coded as in Fig. 1. The diagonal white dashed isodensity lines correspond to the intersections in Fig. 1 of the vertical isochron lines with the black density line. Gravity and quantum uncertainty prevent objects of a given mass from being smaller than their corresponding Schwarzschild radius [Eq. (6)] or Compton wavelength [Eq. (7)]. Schwarzschild black holes lie on the black $m \propto r$ diagonal line which is the lower boundary of the "forbidden by gravity" region. The masses and Compton wavelengths of the top quark (t), Higgs boson (H^o), proton (p), electron (e), and neutrinos (ν) are plotted along the Compton ($m \propto r^{-1}$) diagonal line. Among these, the top quark has the smallest Compton wavelength, because it has the largest mass: 173GeVc^{-2}. The smallest possible object is a Planck-mass black hole indicated by the white dot labeled "instanton" (Ref. 20). Its mass and size are $(m, r) = (m_p, l_p)$. The smallest observable (not yet evaporated) primordial black hole (PBH) that could have survived until today has approximately the same size as a proton (Ref. 21). The large low-mass black dot in the SMBH (super massive black hole) range is the 4×10^6 solar mass black hole at the center of our galaxy (Ref. 22), while the more massive large black dot is Ton 618. The dashed horizontal line at $m = m_p$ emphasizes the orthogonal symmetry of black holes ($m \propto r$) and particles ($m \propto r^{-1}$). Our Universe is represented by the "Hubble radius" and has a mass and size that places it on the black hole line, seemingly suggesting that our Universe is a massive, low-density black hole (Sec. III A). The black rectangle containing neutron stars ("NS"), white dwarfs ("WD"), and brown dwarfs ("BD") indicates the size of the parameter space plotted in Fig. 3. Less comprehensive versions of this plot can be found at Refs. 20 and 23–28. See the supplementary material for the data used to make this plot (Ref. 56).

objects along this isodensity line have the density of water, and because the entire Universe had this density at the end of Big Bang Nucleosynthesis, $\sim 10^3$ s after the big bang. Protons, neutrons, and neutron stars are found along the slope = 3, nuclear density line which is ~14 orders of magnitude more dense than anything made of atoms: $\rho_{nuclear}/\rho_{atomic} \sim 10^{14}$. It is labeled "nuclear 10^{-6} s" because the entire Universe was at this nuclear density a millionth of a second after the big bang.

The largest objects in the upper right are super-clusters of galaxies with densities approximately 20% larger than the current matter density of the Universe. For completeness, we have also plotted the largest known voids. The current matter density is the longest diagonal isodensity line on the right labeled at the top "now 10^{17} s"). This density is the value in Fig. 1 of the black ($\rho_r + \rho_m$) line at $t = now$.

B. Black holes and the zone forbidden by gravity

In Fig. 2, gravity and quantum uncertainty create large forbidden triangular regions where no known objects can exist. All Schwarzschild black holes, from the smallest Planck-

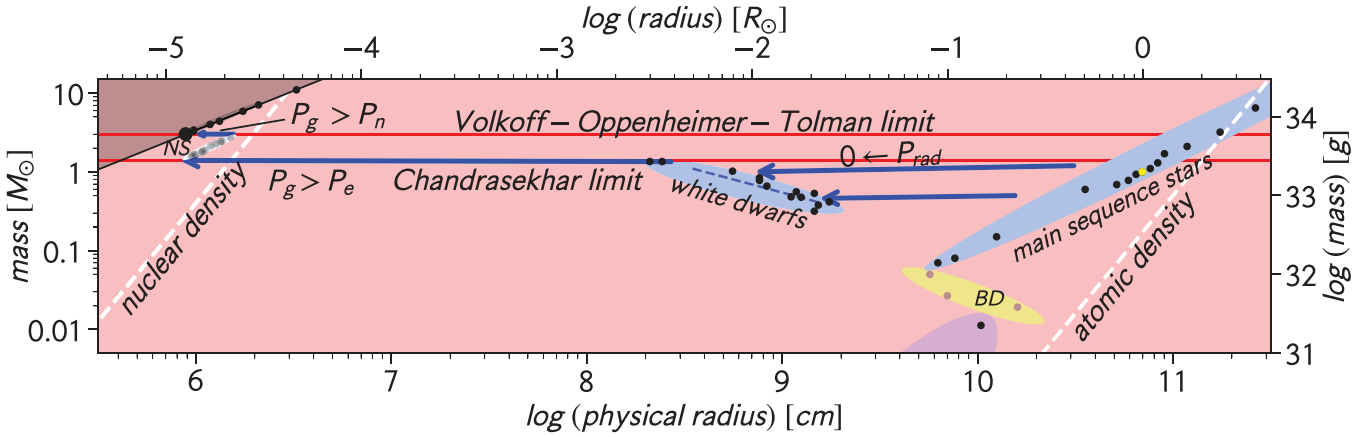

Fig. 3. (Color online) A zoomed-in version of the small rectangle in Fig. 2 containing neutron stars ("NS"), white dwarfs ("WD"), main sequence stars, brown dwarfs ("BD"), and the heaviest mass planet (∼13 Jupiter masses). This plot illustrates the role of degeneracy pressure in the gravitational collapse of stars. Brown dwarfs cannot collapse further due to electron degeneracy pressure, preventing fusion ignition in their cores. They will not become main sequence stars. When main sequence stars (right) run out of fuel they collapse into white dwarfs held up by electron degeneracy pressure. White dwarfs follow the radius-mass relation $r \propto m^{-1/3}$ (blue dashed line) (Ref. 32). When a white dwarf accretes material and its mass approaches the Chandrasekhar limit $\sim 1.4\,M_\odot$ (Ref. 30), it becomes a neutron star "NS" which, with further mass accretion, becomes a black hole "BH," see Sec. II D.

mass instantons to the super-massive black holes (SMBH) at the centers of the largest galaxies, lie on the diagonal $m \propto r$ line labelled "black holes." Black holes lie on this line because the radius and mass of a Schwarzschild black hole are linearly proportional,[29]

$$r_s = \frac{2G}{c^2}\, m. \tag{6}$$

Interestingly, the "Hubble radius" (representing the Universe) also lies on this black hole line (Sec. III A). The "forbidden by gravity" region illustrates that all objects of a given mass are larger than a black hole of that mass, and all objects of a given radius are less massive than a black hole of that radius.

C. Compton wavelengths and the zone forbidden by quantum uncertainty

The effective sizes of small massive particles can be represented by their deBroglie wavelengths: $\lambda_{deB} = \hbar/mv$, where m is the mass of the particle. The higher the velocity v of a particle, the smaller its deBroglie wavelength. In the relativistic limit when $v \to c$, the deBroglie wavelength asymptotes to the smaller Compton wavelength λ_c,

$$\lambda_{deB} = \frac{\hbar}{mv} \overset{v\to c}{\to} \frac{\hbar}{mc} = \lambda_c. \tag{7}$$

The Compton wavelength marks the boundary where relativistic quantum effects become significant. On scales smaller than λ_c, the concept of a single quantum mechanical particle ("object") breaks down and we must switch to a field description in which particle creation and annihilation occur, preventing further spatial localization. In other words, localization of a wave packet to constrain a particle to a size less than its Compton wavelength is prevented by pair-production. Since the Compton wavelength is the lower limit beyond which object size and position are conflated by quantum uncertainty, we take the Compton wavelength as the effective minimum radius of a particle. This produces the $m \propto r^{-1}$ line [Eq. (7)] delimiting the triangular "quantum uncertainty" region in Fig. 2.

In addition to composite particles, we also plot fundamental structureless particles, e.g., quarks and leptons. As examples, we plot the top quark, electron, and neutrinos. These all lie along the Compton wavelength boundary. For completeness, we would also like to plot massless photons. However, since the Compton wavelength of a massless particle (photons, gluons, and gravitons) is infinity, we plot photons at $(m_{eff}, size) = (E/c^2, \lambda_\gamma)$ where their angular wavelengths $\lambda_\gamma = \hbar c/E$. Thus, photons of the entire electromagnetic spectrum can be plotted. They fall along the Compton limit line since $m_{eff} \sim \lambda_\gamma^{-1}$. The narrow rainbow at $E \sim 10^{-9}$ GeV is the entire visible spectrum, while the entire electromagnetic spectrum extends from the shortest wavelength gamma ray $\lambda_\gamma = l_p$ to the longest radio waves extending off the plot beyond the size of the observable Universe.

D. Stellar mass black holes and degeneracy pressure

Figure 3 illustrates some important features of stellar evolution. When a main sequence star (right side of Fig. 3) runs out of fuel, it can no longer maintain the thermal radiation pressure P_{rad}, to counteract gravitational pressure P_g: $(P_{rad} \to 0 < P_g)$. It collapses and becomes a white dwarf held up mostly by electron degeneracy pressure ($P_e \sim P_g$). Counter-intuitively, more massive white dwarfs are smaller than less massive ones because as gravity compresses massive particles, temperatures increase, velocities increase, and the deBroglie wavelengths λ_{deB} of the electrons decrease and at relativistic energies asymptote to their smaller Compton wavelengths [Eq. (7)]. Gravity cannot compress the sizes of the electrons to be less than their Compton wavelengths. This size limit is the source of the electron degeneracy pressure that holds up white dwarfs. However, if a white dwarf can accrete more mass than the Chandrasekhar limit $\sim 1.4\,M_\odot$,[30] gravitational pressure at the center is enough to overcome electron degeneracy pressure ($P_g > P_e$). Electrons are pushed into protons producing neutrons, and thus, white dwarfs collapse into neutron stars held up by neutron degeneracy pressure.[31] If a neutron star can accrete more mass than the Volkoff–Oppenheimer–Tolman limit of $\sim 3\,M_\odot$,[31]

the star will continue to collapse, overcoming neutron degeneracy pressure and collapsing into a black hole.

III. SOME FUNDAMENTAL QUESTIONS

A. Is the Universe a black hole?

In our expanding Universe, Hubble's law relates the recession velocities to the distance: $v_{rec} = H\,r$. At a specific distance r_H called the Hubble radius, the recession velocity is equal to the speed of light,

$$r_H = \frac{c}{H}. \tag{8}$$

The Hubble volume is a sphere of radius r_H centered on us and is often taken as the size of the Universe. At present, $r_H \approx 14\,\text{Gly}$.[33] In Fig. 2, the most massive point on the black hole line is labeled "Hubble radius" at the point (m_U, r_H) where the mass of the Universe is the critical density times its volume: $m_U = \rho_c\,(4/3)\,\pi\,r_H^3$.

Using Eq. (6), we can write the density of a black hole as

$$\rho_{BH} = \frac{m}{V} = \frac{m}{\frac{4}{3}\pi\,r_s^3} = \frac{m}{\frac{4}{3}\pi}\left(\frac{c^2}{2Gm}\right)^3 \tag{9}$$

$$= \frac{3c^6}{32\pi G^3}\,m^{-2}. \tag{10}$$

Thus, $\rho_{BH} \propto m^{-2}$ and the more massive the black hole, the lower its density. This can also be seen in Fig. 2, where the most massive black holes are on the lowest density isodensity lines. In particular, when the size of a black hole is the size of the Universe ($r_s = r_H$), we can use Eqs. (6) and (8) in Eq. (10) to obtain

$$\rho_{BH} = \frac{3H^2}{8\pi G} = \rho_c, \tag{11}$$

where ρ_c is the critical density. Thus, a Schwarzschild black hole the same size as our Universe has the same mass and density as our Universe. This seems to suggest that the entire Universe is a black hole. Although this idea has been explored in Refs. 34–37, Fig. 4 illustrates why this is not the case.

B. Where exactly do the black hole and Compton boundaries cross?

In Fig. 2, the black hole diagonal line has a slope of $+1$ since $\log(m) \propto \log(r)$ [Eq. (6)]. The diagonal line of the Compton wavelengths has a slope of -1 since $\log(m) \propto -\log(r)$ [Eq. (7)]. Thus, these two lines are orthogonal and should cross at the instanton which is "a black hole whose Compton wavelength is equal to its Schwarzschild radius."[28] We want to verify that this instanton crossing point happens at (l_p, m_p). The Compton wavelength [Eq. (7)] of a Planck-mass particle is

$$\lambda_c(m_p) = \frac{\hbar}{m_p c} = \frac{\hbar}{c}\left(\frac{G}{\hbar c}\right)^{1/2} = \left(\frac{\hbar G}{c^3}\right)^{1/2} = l_p, \tag{12}$$

where l_p is the Planck length and the Planck mass $m_p = (\hbar c/G)^{1/2}$. Thus, the Compton wavelength of a Planck-mass particle equals the Planck length: $\lambda_c(m_p) = l_p$. However, what about the black hole diagonal line? Is the Schwarzschild radius of a Planck-mass black hole equal to the Planck length?

$$r_s(m_p) = \frac{2\,G\,m_p}{c^2} = \frac{2\,G}{c^2}\left(\frac{\hbar c}{G}\right)^{1/2} = 2\left(\frac{\hbar G}{c^3}\right)^{1/2} = 2\;l_p. \tag{13}$$

There is an unexpected extra factor of 2. Thus, the two diagonal lines do not cross at exactly (l_p, m_p). Instead we have the radius of a Planck-mass black hole equal to twice the Compton wavelength of a Planck-mass particle (see p. 225 of Ref. 38).

Insight into this factor of 2 may be found by considering not the simplified case of a non-rotating Schwarzschild black hole but the more general case of a rotating Kerr black hole. For convenience, we first define a length proportional to the angular momentum L per unit mass $r_L = (L/m)\,c$ [Ref. 16, p 60, Eq. (2.100)]. Then, in the equatorial plane of the rotating black hole, we have singularity solutions

$$r_\pm = \frac{r_s}{2} \pm \left[\left(\frac{r_s}{2}\right)^2 - r_L^2\right]^{1/2}, \tag{14}$$

where the $\pm$ indicates there are two solutions and the angular momentum parameter r_L can take on values in the range $r_L \in [0, r_s/2]$. These two solutions are called the inner (Cauchy) horizon and the outer horizon. For $r_L = 0$ (non-rotating), we recover the Schwarzschild solution $r_+ = r_s$ as the outer horizon. However, we also have a solution for the inner (Cauchy) horizon $r_- = 0$ that is often ignored. Importantly, $r_+ < r_s$ for all non-zero values of r_L. For all values of r_L, the average of the two solutions equals $r_s/2$. For a

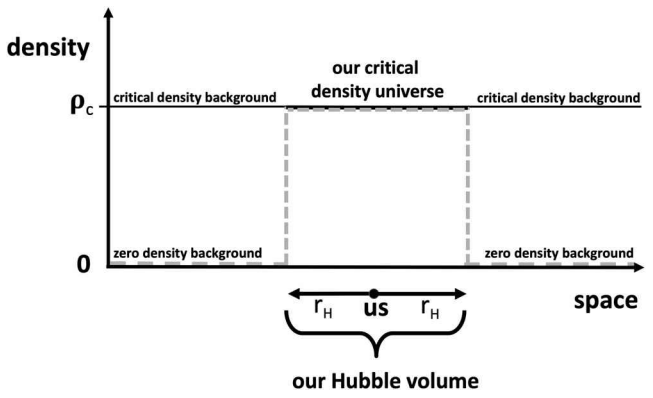

Fig. 4. We can imagine our Universe being surrounded by two different background densities: (1) zero density (dashed grey lines) or (2) a critical density with the same density as our Universe (horizontal black line). If our critical density Universe with "us" in the middle is surrounded by a zero density flat Minkowski spacetime then we can use the Schwarzschild metric to conclude that we are living in a black hole and headed for a big crunch. However, if the Universe outside the Hubble radius "r_H" has the same critical density as the inside, then the Friedmann–Robertson–Walker metric tells us we are living in a flat universe and we cannot use the Schwarzschild metric (Ref. 29) to describe our situation because the Schwarzschild radius of a black hole has been calculated under the assumption that the black hole is surrounded by empty $\rho = 0$ flat Minkowski spacetime.

maximally rotating black hole, the two horizons merge, $r_\pm = r_s/2$. The inner (Cauchy) and outer horizons for a maximally rotating Planck-mass black hole are both equal to the Planck length: $r_\pm = l_p = \lambda_c(m_p)$.

The Reissner–Nördstrom metric for a charged (non-rotating) black hole leads to analogous solutions: maximally charged Planck-mass black holes have $r_\pm(m_p) = r_s/2 = l_p$.[39,40] Thus, the most fundamental length in both the Kerr and Reissner-Nördstrom metrics for a Planck-mass black hole is the Planck length $l_p = r_s/2$. In Fig. 2, if we had represented the radius of a black hole by the average of the outer horizon and the inner (Cauchy) horizon: $r_{BH} = (r_+ + r_-)/2$, the black hole line and the Compton wavelength line would cross exactly at the instanton point (l_p, m_p).

IV. DISCUSSION

The Planck-mass instanton is the smallest mass a black hole can have without entering the region of quantum uncertainty. Instantons seem to be the smallest objects in the Universe (white dot in Fig. 2).[20] On the upper left side of Fig. 1, we have assumed the initial condition that the Universe started out at the Planck time with the Planck density and Planck temperature. In Fig. 2, the intersection point of the vertical white line at the Planck length and the diagonal dashed white line at the Planck density is an instanton. The Hawking temperature of an instanton is the Planck temperature.[16] Thus, we have assumed that the initial conditions of the Universe are that of an instanton. Instantons seem to be an essential ingredient for quantum cosmology, and their study is an active field of research that is beyond the scope of this paper.[20,26,27,41–47]

It is possible that some kind of quantum degeneracy pressure holds up the core of a black hole and prevents it from becoming a Schwarzschild singularity.[48,49] If so, the cores of black holes could be Planck-density objects located in the "forbidden by gravity" region along the Planck isodensity line. Or the cores could have sizes corresponding to the inner Cauchy horizons [r_- in Eq. (14)], also located in the "forbidden by gravity" region.

How can we interpret the doubly forbidden black triangular region labeled "QG" (quantum gravity) on the left side of Fig. 2? What does it mean to be doubly forbidden? In this region, the size r of an object violates both general relativity: $r < r_s = 2Gm/c^2$ and quantum uncertainty: $r < \lambda_c = \hbar/mc$. In terms of mass m, gravity and quantum uncertainty prevent the mass of an object from satisfying

$$\frac{rc^2}{2G} < m < \frac{\hbar}{rc}. \tag{15}$$

The Compton limit involves only the Heisenberg uncertainty principle. However, as we approach the instanton, a term relevant to gravitational effects also contributes to the uncertainty. Including this gravitational term extends the Heisenberg uncertainty principle into what is known as the generalized uncertainty principle.[27,50,51]

Carr and collaborators have raised some fundamental issues about the orthogonal symmetry of the black hole line ($m \propto r$) and Compton line ($m \propto r^{-1}$) around the horizontal dashed line in Fig. 2. They refer to this symmetry as the "Compton–Schwarzschild correspondence," which plays a fundamental role in quantum gravity.[20,27,51,52]

The history of objects in the Universe can be seen as a history of condensations of composite objects from an undifferentiated background. Although composite objects condensed when the binding energy of the object exceeded the background energy, notice in Fig. 2 that no known objects condense before the electroweak (EW) energy scale at 10^{-10} s, because the binding energies of all known composite objects are less than the background energy at these early times. Perhaps there are composite objects embedded in the quark-gluon plasma (QGP) held together by the unified strong, weak and electromagnetic forces. Two important open questions are: What were the first composite objects? and If we consider virtual particles to be objects, where do they belong in the diagram?

V. CONCLUSIONS

There is a long inspiring pedagogical tradition in physics of putting everything into one log-log plot. This tradition includes a logarithmic overview of all space (powers of ten[53]), a logarithmic overview of all time (time in powers of ten[54]), and "the complete history of the Universe" (Fig. 3.7 of Ref. 1). Okun's "the physical theories cube" (Fig. 2 of Ref. 55) is a powerful pedagogical tool that enables us to imagine the variation of three fundamental constants $1/c$, G, and $\hbar$. Each of the eight vertices of his cube corresponds to different physical theories.

Here, we provide an overview of the history of the Universe and the sequence of composite objects (e.g., protons, planets, galaxies) that condensed out of the background as the Universe expanded and cooled. We describe the role of the effective number of relativistic degrees of freedom (g_*) needed to understand the thermal history of the Universe during the first few minutes after the big bang. We compute and plot the background density and temperature of the Universe (Fig. 1). To extrapolate into the first billionth of a second, we make some common, explicit, but speculative assumptions.

We then make the most comprehensive pedagogical plot of the masses and sizes of all the objects in the Universe (Fig. 2). This plot draws attention to the unphysical regions forbidden by general relativity and quantum uncertainty—regions bounded by black holes and the Compton limit. The Compton limit creates an ambiguous region beyond which object size and position are conflated by quantum uncertainty, thus undermining the classical notion that the size of an object can be arbitrary small. Figure 2 also helps navigate the relationship between gravity and quantum mechanics and helps formulate some fundamental questions about the limits of physics: How can we interpret the regions forbidden by general relativity and quantum uncertainty? How should we interpret the fact that the two boundaries of the forbidden regions intersect at the instanton (Planck-mass black holes)? Are instantons the smallest possible objects? Do their size, density and temperature make them the best candidates for the initial conditions of the Universe (Fig. 1)? Is the Schwarzschild radius the minimum size for an object of a given mass? Or might the non-singular cores of black holes be objects with the Planck density?

AUTHOR DECLARATIONS

Conflict of Interest

The authors have no conflicts to disclose.

[a]ORCID: 0000-0003-2047-1558.
[b]ORCID: 0000-0001-5474-3561.

[1]E. Kolb and M. S. Turner, *The Early Universe. Frontiers in Physics* (Avalon Publishing, New York, 1994).
[2]National Research Council, *Connecting Quarks with the Cosmos: Eleven Science Questions for the New Century* (National Academies Press, Washington, DC, 2003).
[3]S. Weinberg, *Cosmology* (Oxford U.P., Oxford, 2008).
[4]F. J. Dyson, *A Many-Colored Glass: Reflections on the Place of Life in the Universe* (University of Virginia Press, Charlottesville, VA, 2007), Chap. 4, p. 63.
[5]M. S. Turner, "The road to precision cosmology," Annu. Rev. Nucl. Part. Sci. **72**(1), 1–35 (2022).
[6]C. A. Egan and C. H. Lineweaver, "A larger estimate of the entropy of the universe," Astrophys. J. **710**(2), 1825–1834 (2010).
[7]L. Husdal, "On effective degrees of freedom in the early universe," Galaxies **4**(4), 78 (2016).
[8]S. Borsányi *et al*., "Calculation of the axion mass based on high-temperature lattice quantum chromodynamics," Nature **539**(7627), 69–71 (2016).
[9]Planck Collaboration, "Planck 2018 results. VI. Cosmological parameters," Astron. Astrophys. **641**, A6 (2020).
[10]J. J. Atick and E. Witten, "The Hagedorn transition and the number of degrees of freedom of string theory," Nucl. Phys. B **310**(2), 291–334 (1988).
[11]Roger Penrose, *Cycles of Time: An Extraordinary New View of the Universe* (Random House, New York, 2010).
[12]P. A. Zyla *et al*., "Review of Particle Physics," Prog. Theor. Exp. Phys. **2020**, 083C01.
[13]A. H. Guth, "Inflationary universe: A possible solution to the horizon and flatness problems," Phys. Rev. D **23**(2), 347–356 (1981).
[14]A. D. Linde, "A new inflationary universe scenario: A possible solution of the horizon, flatness, homogeneity, isotropy and primordial monopole problems," Phys. Lett. B **108**(6), 389–393 (1982).
[15]A. Albrecht, P. J. Steinhardt, M. S. Turner, and F. Wilczek, "Reheating an inflationary universe," Phys. Rev. Lett. **48**(20), 1437–1440 (1982).
[16]J. A. Peacock, *Cosmological Physics* (Cambridge U.P., Cambridge, 2010).
[17]E. Harrison, *Cosmology: The Science of the Universe*, 2nd ed. (Cambridge U.P., Cambridge, 2022).
[18]S. M. Carroll, *Spacetime and Geometry* (Cambridge U.P., Cambridge, 2019).
[19]D. J. Fixsen, "The temperature of the cosmic microwave background," Astrophys. J. **707**(2), 916–920 (2009).
[20]B. J. Carr and M. J. Rees, "The anthropic principle and the structure of the physical world," Nature **278**(5705), 605–612 (1979).
[21]S. W. Hawking, "Particle creation by black holes," Commun. Math. Phys. **43**(3), 199–220 (1975) [Erratum: Commun. Math. Phys. **46**, 206–208 (1976)].
[22]R. Abuter, A. Amorim, M. Bauböck, J. P. Berger, H. Bonnet, W. Brandner, Y. Clénet, V. Coudé du Foresto, P. T. de Zeeuw, J. Dexter, G. Duvert, A. Eckart, F. Eisenhauer, N. M. Förster Schreiber, P. Garcia, F. Gao, E. Gendron, R. Genzel, O. Gerhard, S. Gillessen, M. Habibi, X. Haubois, T. Henning, S. Hippler, M. Horrobin, A. Jiménez-Rosales, L. Jocou, P. Kervella, S. Lacour, V. Lapeyrère, J.-B. Le Bouquin, P. Léna, T. Ott, T. Paumard, K. Perraut, G. Perrin, O. Pfuhl, S. Rabien, G. Rodriguez Coira, G. Rousset, S. Scheithauer, A. Sternberg, O. Straub, C. Straubmeier, E. Sturm, L. J. Tacconi, F. Vincent, S. von Fellenberg, I. Waisberg, F. Widmann, E. Wieprecht, E. Wiezorrek, J. Woillez, S. Yazici, and GRAVITY Collaboration, "A geometric distance measurement to the galactic center black hole with 0.3% uncertainty," Astron. Astrophys. **625**, L10 (2019).
[23]R. V. Wagoner and D. Goldsmith, *Cosmic Horizons: Understanding the Universe* (Stanford Alumni Association, Stanford, CA, 1982).
[24]M. Rees, *Perspectives in Astrophysical Cosmology* (Cambridge U.P., Cambridge, 1995).
[25]M. Rees, *Our Cosmic Habitat* (Princeton U.P., Princeton, 2001).
[26]J. R. Primack and N. E. Abrams, *The View from the Center of the Universe: Discovering Our Extraordinary Place in the Cosmos* (Penguin Publishing Group, New York, 2007).
[27]M. J. Lake and B. J. Carr, "Does Compton-Schwarzschild duality in higher dimensions exclude TeV quantum gravity?," Int. J. Mod. Phys. D **27**(16), 1930001–1930167 (2018).
[28]M. Livio and M. Rees, "Fine-tuning, complexity, and life in the multiverse," *Fine-tuning in the Physical Universe* (Cambridge U.P., Cambridge, 2020), pp. 1–19.
[29]K. Schwarzschild, "On the gravitational field of a mass point according to Einstein's theory," Sitzungsber. Preuss. Akad. Wiss. Berlin **1916**, 189–196.
[30]S. Chandrasekhar, "The maximum mass of ideal white dwarfs," Astrophysical J. **74**, 81–82 (1931).
[31]J. R. Oppenheimer and G. M. Volkoff, "On massive neutron cores," Phys. Rev. **55**(4), 374–381 (1939).
[32]R. K. Pathria, *Statistical Mechanics* (Elsevier, Amsterdam, 2016).
[33]T. M. Davis and C. H. Lineweaver, "Expanding confusion: Common misconceptions of cosmological horizons and the superluminal expansion of the universe," Publ. Astron. Soc. Aust. **21**(1), 97–109 (2004).
[34]R. K. Pathria, "The universe as a black hole," Nature **240**(5379), 298–299 (1972).
[35]I. Dymnikova, "Universes inside a black hole with the de Sitter interior," Universe **5**(5), 111 (2019).
[36]E. Gaztañaga, "Inside a black hole: The illusion of a big bang," <https://hal.science/hal-03106344v7> (2021).
[37]E. Gaztanaga, "How the big bang ends up inside a black hole," Universe **8**(5), 257 (2022).
[38]G. Börner, *The Early Universe: Facts and Fiction* (Springer Science & Business Media, Berlin, 2013).
[39]A. P. Lightman, W. H. Press, R. H. Price, and S. A. Teukolsky, *Problem Book in Relativity and Gravitation* (Princeton U.P., Princeton, 2017).
[40]Wikipaedia, "Reissner-Nordström metric," <https://en.wikipedia.org/wiki/ReissnerNordström_metric>, accessed on February 8, 2023.
[41]S. Hawking, "Gravitationally collapsed objects of very low mass," Mon. Not. R. Astron. Soc. **152**(1), 75–78 (1971).
[42]S. Coleman and F. De Luccia, "Gravitational effects on and of vacuum decay," Phys. Rev. D **21**(12), 3305–3315 (1980).
[43]S. W. Hawking and I. L. Moss, "Supercooled phase transitions in the very early universe," Phys. Lett. B **110**(1), 35–38 (1982).
[44]S. W. Hawking and N. Turok, "Open inflation without false vacua," Phys. Lett. B **425**(1-2), 25–32 (1998).
[45]H. Firouzjahi, "Primordial universe inside the black hole and inflation," preprint arXiv:1610.03767 (2016).
[46]*Fine-tuning in the Physical Universe*, edited by M. Hicks, D. Sloan, R. Alves Batista, and R. Davies (Cambridge U.P., Cambridge, 2020).
[47]B. J. Carr, K. Kohri, Y. Sendouda, and J. Yokoyama, "Constraints on primordial black holes," Rep. Prog. Phys. **84**(11), 116902 (2021).
[48]L. H. Ford, "The classical singularity theorems and their quantum loopholes," Int. J. Theor. Phys. **42**(6), 1219–1227 (2003).
[49]N. Huggett and K. Matsubara, "Lost horizon?–Modeling black holes in string theory," Eur. J. Philos. Sci. **11**(3), 70 (2021).
[50]R. J. Adler and D. I. Santiago, "On gravity and the uncertainty principle," Mod. Phys. Lett. A **14**(20), 1371–1381 (1999).
[51]B. J. Carr, "The black hole uncertainty principle correspondence," Springer Proc. Phys. **170**, 159–167 (2016).
[52]M. J. Lake and B. J. Carr, "The Compton-Schwarzschild correspondence from extended de Broglie relations," J. High Energy Phys. **2015**(11), 105.
[53]P. Morrison and P. Morrison, *Powers of Ten: About the Relative Size of Things in the Universe* (Scientific American Books, New York, 1982).
[54]G. t'Hooft and S. Vandoren, *Time in Powers of Ten: Natural Phenomena and Their Timescales* (World Scientific, Singapore, 2014).
[55]L. B. Okun, "The fundamental constants of physics," Sov. Phys. Usp. **34**(9), 818–826 (1991).
[56]See supplementary material online for data and citations used in Figs. 2 and 3.